

# NEW DEVELOPMENTS AND STATUS OF XAIRA, THE NEW MICROFOCUS MX BEAMLINE AT THE ALBA SYNCHROTRON

N. González<sup>†</sup>, J. Juanhuix, J. Nicolás, D. Garriga, M. Quispe, A. Crisol, I. Sics, C. Colldelram  
ALBA Synchrotron Light Source, Cerdanyola del Vallés, Spain

## Abstract

The new BL06-XAIRA microfocus macromolecular crystallography beamline at ALBA synchrotron is currently under commissioning and foreseen to enter into user operation in 2024. The aim of XAIRA is to provide a 4 – 14 keV, stable, high flux beam, focused to  $3 \times 1 \mu\text{m}^2$  FWHM. The beamline includes a novel monochromator design combining a cryocooled Si(111) channel-cut and a double multilayer diffracting optics for high stability and high flux; and new mirror benders with dynamical thermal bump and figure error correctors. In order to reduce X-ray parasitic scattering with air and maximize the photon flux, the entire end station, including sample environment, cryostream and detector, is enclosed in a helium chamber. The sub-100 nm SoC diffractometer, based on a unique helium bearing goniometer also compatible with air, is designed to support fast oscillation experiments, raster scans and helical scans while allowing a tight sample to detector distance. The beamline is also equipped with a double on-axis visualization system for sample imaging at sub-micron resolutions. The general status of the beamline is presented here with particular detail on the in-house fully developed end station design.

## INTRODUCTION

ALBA is a synchrotron light source located in the Barcelona area hosting ten operating beamlines, with four more beamlines in design or construction phases. Long-term plans include the upgrade of the facility to a 4th generation source together with major upgrades of the existing beamlines.

BL06-XAIRA is a new microfocus macromolecular crystallography (MX) beamline currently in commissioning, expecting first users along 2024. The beamline is designed to deliver high quality data from micron-sized and/or poorly diffracting crystals from oscillation and fixed-target MX experiments, as well as from experiments at low photon energies exploiting the anomalous signal of the metals naturally occurring in proteins (native phasing), which is enhanced in the case of small crystals. To this aim XAIRA is foreseen to provide a  $\sim 4 - 14$  keV,  $3 \times 1 \mu\text{m}^2$  FWHM ( $h \times v$ ), which can be slit down to  $1 \times 1 \mu\text{m}^2$ , with a flux of  $> 10^{13}$  ph/s/250 mA at 1 Å wavelength (12.4 keV).

The entire end station, that is detector, cryostream, diffractometer and sample conditioning elements, is enclosed in a helium chamber to provide optimal conditions for experiments at low energies as low as 3 keV. The system allows the recovery of the helium and is compatible with standard operation in air.

## BEAMLINE DESCRIPTION

The optical design of the beamline was first described in the SRI2018 conference in Taiwan [1]. The beamline is fed by a permanent magnet in-vacuum undulator, IVU19, with a magnetic period of 19.9 mm and a minimum gap of 5.2 mm [2]. The high power produced by the undulator, up to 4.3 kW at 250 mA, and the absence of vacuum windows to maximize the flux at low photon energies impose severe constraints on the cooling systems of the optical elements up to the monochromator. To mitigate this, the aperture of the front-end moveable masks is set to limit the power delivered to the beamline optics to 1.3 kW.

The complete beamline layout is shown in Figure 1. The beam is focused by two horizontal focusing mirrors, the horizontally prefocusing (HPM) and focusing (HFM) mirrors, and a vertically focusing mirror (VFM), the two latter mounted as a KB mirror pair. The mirrors are elliptically bent in the meridional direction by ALBA mirror benders, which provide sub-nanometric resolution and stability and allow correcting the wavefront deformations caused by static or dynamic effects such as long-period figure errors and thermal bumps [3]. High-precision slits (HSS) are placed at the focal position of the HPM to reduce the horizontal beam size, so that it can be further focused by the HFM to  $1 \mu\text{m}$  FWHM at the sample position.

The energy is selected using a cryogenically cooled monochromator that combines a narrow gap, 4.5 mm, channel-cut monochromator (CCM) and a double multilayer monochromator (DMM) mounted on the same Bragg axis. The geometry has been optimized to switch from one to another without the need of any translations. The beam diagnostics include one cooled and 4 non-cooled fluorescence screens (FS) [4] to monitor the beam profile and shape, and two 20  $\mu\text{m}$  thickness CVD diamond XBPMs from Cividec to position and measure the incoming beam flux and two sets of slits to reduce the beam divergence.

The sample is located just 1 m downstream the last KB mirror, the HFM, in a vertically oriented goniometer. The entire end station, which includes the diffractometer, the detector, the cryostream and the sample visualization system, among others, is enclosed in a helium chamber, which can also be opened to air. In between the KB chamber and the helium chamber, the Beam Conditioning Elements (BCEM) enclose a fast shutter, a 4-blade slits set, an XBPM and a beam diagnostic unit with a YAG:Ce screen and a phodiode. The vacuum-helium or air interface between the BCEM chamber and the end station is maintained with a 10  $\mu\text{m}$  thickness and 2 mm diameter diamond window. Besides, so as to monitor the beam stability at sample position, the two XBPMs include Q-Tools

<sup>†</sup> ngonzalez@cells.es

Content from this work may be used under the terms of the CC-BY-4.0 licence (© 2023). Any distribution of this work must maintain attribution to the author(s), title of the work, publisher, and DOI

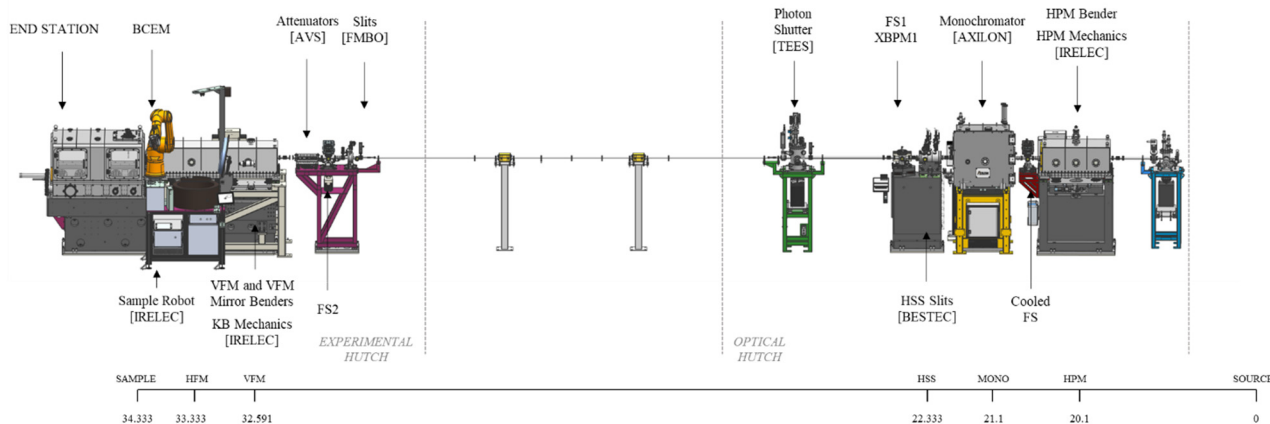


Figure 1: XAIRA beamline layout. Manufacturers are marked in brackets.

interferometers for vertical position feedback. Additionally, the HFM and VFM mirrors also include three interferometers each, pointing directly at the mirror surface and giving a direct reading of the mirror pitch and position. Three more interferometers will be used to monitor the sample position.

## WHITE/PINK BEAM OPTICAL COMPONENTS

### Horizontal Prefocusing Mirror (HPM)

The HPM consists on a silicon substrate of  $40 \times 30 \times 670 \text{ mm}^3$  ( $W \times H \times L$ ) mounted on a horizontally deflecting ALBA mirror bender. The optical surface is limited to 450 mm length although the mirror acceptance is larger. The nominal applied forces, 438 N (upstream) and 623 N (downstream), allow to focus the beam at the HSS placed 2.233 m downstream. The power load on the HPM is limited vertically by the front-end aperture, and horizontally by the acceptance of the mirror and the cooled mask placed before the mirror. The resulting nominal absorbed power load is 154 W at 250 mA, which results in a moderate peak power density of  $\leq 0.22 \text{ W/mm}^2$ . These input conditions allow using a water-cooling system applied at the sides of the mirror. Still, the absorbed power induces a significant increase of the temperature and an expansion of the optical surface, thus, a cooling system to keep the mirror at a stable temperature while allowing the mirror bending was required.

The cooling system design is based on the method developed at SLAC [5], which uses a 100  $\mu\text{m}$  eutectic InGa layer between the mirror and the silicon pads attached to the copper pads. Two independent stainless-steel tubes are brazed to these 500 mm copper pads. The pads are nickel plated in order to avoid Cu-InGa issues. The silicon pads, five on each side, are clamped to the copper pads with 50  $\mu\text{m}$  Indium foils in between. The complete setup is shown at Figure 2. The difference of using Indium foils instead of InGa in this union was calculated by thermal FEA and no big impact was observed. The thermal conductivity of the system was validated at the optics lab before the installation at the beamline circulating hot water through the

pipes and visualizing the temperature increase using a precision infrared camera (Optris PI640).

In-depth metrology measurements were done on the mirror bender, with and without the cooling, in order to evaluate its effect on the bender performance. The results show the performance was not affected by the shear forces of the 100  $\mu\text{m}$  eutectic InGa layer, as shown at Table 1.

Table 1: Bender Performance

Parameter	Value
Bender Error	0.023 $\mu\text{rad rms}$
Radius repeatability $\Delta R/R$	0.0076 %
Radius Stability (14h)	0.0054 % rms
Radius Resolution	$\leq 0.0371 \%$
Slope Error	$\leq 0.258 \mu\text{rad rms}$
Height Error	1.56 nm rms

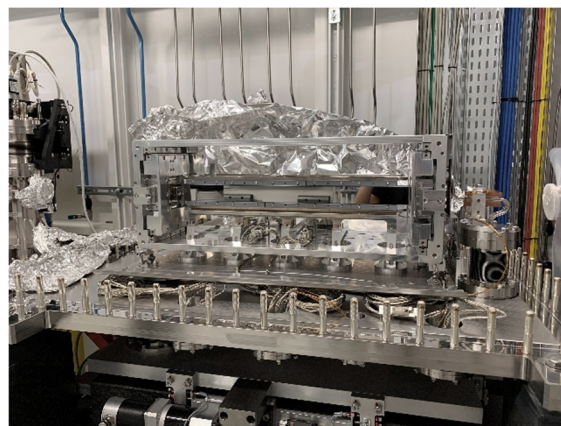


Figure 2: Picture of the HPM Bender at the beamline.

The cooling system was validated by illuminating the full optical length of the mirror at the maximum power delivered by the undulator. The mirror temperature increased with the front-end vertical aperture (Figure 3). At maximum tested aperture, beyond nominal conditions, the mirror absorbs 211 W power (incoming 604 W) while the mirror temperature rises to 30  $^{\circ}\text{C}$ , as predicted by FEA. Mirror temperature can be seen in the next Figure 3.

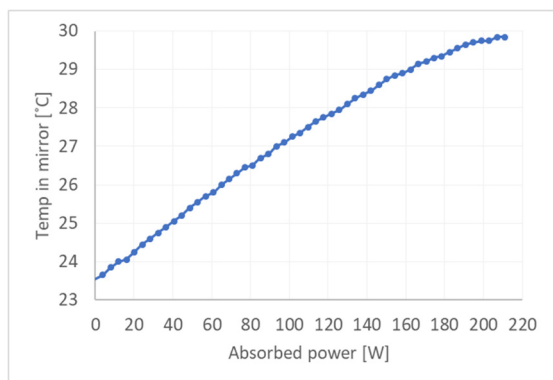


Figure 3: HPM Temperature vs. absorbed power.

### Monochromator

The monochromator of XAIRA is based on a novel concept that combines a channel cut monochromator (CCM) and a double multilayer monochromator in a single mount. The Bragg axis is placed 2.3 mm underneath the first optical surface, both for the multilayer and the channel cut crystal, and intersects the beam axis. In this configuration, the center of the beam travels along the crystals surface depending only from the Bragg angle,  $\theta$ . Due to the relatively small grazing incidence angle of the multilayers (ML) in the hard X-ray compared to the channel cut, the beam positions for the two diffracting surfaces do not overlap in the range of 4 – 14 keV for the CC and 6 – 14 keV for a ML with a d spacing of 26 Å. Therefore, it is feasible, from the geometrical point of view, to optimize the dimensions, so as to have the two surfaces in the same plane and change from one optics to another just changing the Bragg rotation angle without the need of any translations. The sketch is shown in Figure 4.

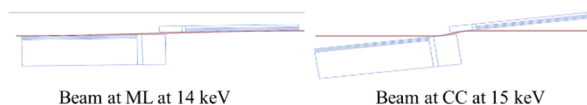


Figure 4: Conceptual Sketch of the CCM/DMM monochromator. Bragg angle 1 deg (left) and 7.6 deg (right).

The two optics, a Si(111) channel-cut crystal and a double Mo/B<sub>4</sub>C multilayer are cryogenically cooled by a common pair of clamped cooling pads. The optimization of the cooling internal geometry was carefully done by CFD and thermal FEA simulations in order to make the LN<sub>2</sub> flow as uniform as possible and minimize turbulences so as to maximize vibrational stability while maximizing the cooling capacity. Considering that the absorbed power is around 235 W at worst case, the cooling performance is especially important at low energies of the CC, with an incidence angle of around 29 deg and a peak power density of 20 W/mm<sup>2</sup>. The influence of the LN<sub>2</sub> cooling on the MM was also a main concern. Mo/B<sub>4</sub>C was found to be the most suitable coating material for cryogenic temperatures and the cooling pads were also optimized so that the thermal cycling on the MM substrate was reduced to just a few kelvins in working conditions. Another critical aspect was the assembly of the optical substrates. While the clamping pressure is a key parameter in order to have a good thermal

### PHOTON DELIVERY AND PROCESS

#### Beamlines

conductance, an overpressure induced surface deformations on the MM optical surface. The clamping procedure was carefully done measuring the optical surfaces with a Fizeau interferometer while increasing the pressure.

The design and construction of the monochromator mechanics was done by AXILON. First commissioning tests with beam have proven that the concept works fine, being able to change from one substrate to another just rotating the Bragg axis in less than 1.3 min (limited by the rotation speed) while keeping the horizontal beam position and energy. Beam images can be seen in Figure 5.

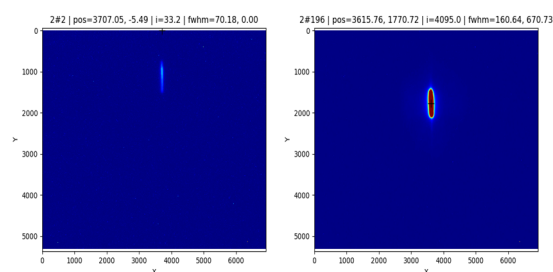


Figure 5: Beam at FS1, downstream the monochromator, for the CC (left) and ML (right), both at 7.3 keV.

## END STATION

### General Layout

The end station of XAIRA is composed by the following components which can be shown in Figure 6.

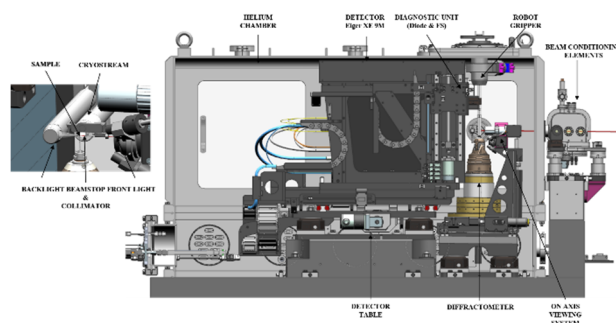


Figure 6: End Station Components.

- The Beam Conditioning Elements (BCEM), is the chamber located just downstream the KB and upstream the helium chamber. It contains a fast shutter, 4-blade slits, a XPBM and a diagnostic unit, all driven by SMARACT piezoguides, in a tight space of 150 mm. The chamber ends in a 10 μm 2 mm diameter window that separates the ultra-high vacuum section from the end station, at atmospheric pressure.
- The cryostream, Cryocool – G2b. Manufactured by Cryo Industries America, it provides continuous cold gas of helium or nitrogen in order to maintain the sample at cryogenic temperatures.
- The detector and detector table. The detector, a fast photon counting pixel Dectris EIGER2 XE 9M, is mounted over a longitudinal and transversal very stable translation table. The detector, which can also work both in helium and in air, can be located as close

as 70 mm to the sample for high resolution experiments. In addition, the detector cover frame includes a fast in/out diagnostic unit to image the beam and measure flux at the detector position.

- The sample loading robot. The robot, manufactured by IRELEC, is capable of loading and unloading the samples at cryogenic temperatures. The double gripper has been customized with a sealing interface in order to minimize the helium leakage and make it compatible with the helium chamber, which has a valve on top to allow the gripper entrance.
- The sample illumination system and, beamstop and collimator assembly, from ARINAX. A front light, mounted on the on-axis sample viewing system and a removable backlight system illuminate the sample. A 500  $\mu\text{m}$ -thick beamstop is mounted and pre-aligned with a 100  $\mu\text{m}$  cleaning aperture capillary. The assembly is mounted on the on axis viewing (OAV) system so that they move together to follow the beam excursion but they can be retracted, for sample loading.

### Helium Chamber

The Helium chamber is located and seals against the end station granite with Viton rings. The chamber is split in two parts, the bottom part, which will always remain installed, contains all the electrical feedthroughs and piping interfaces, manufactured as for UHV conditions to minimize helium leaks. The top part, removable, includes several doors to access for maintenance, the robot interface on the top with a get valve and the interfaces required by the helium recovery circuit [6].

### Diffractometer

Due to the tight space constrains (only 70 mm from sample to detector) and the demanding performance requirements: Sphere of Confusion (SoC)  $\leq 100$  nm, resolution of 0.05 mdeg and maximum speed of 360 deg/s, together with the requirement of having to be compatible both with helium and air, it was decided to fully develop the diffractometer in house. The vertically oriented goniometer,  $\Omega$ , is mounted on a high stability XY stage, that allows aligning the rotation axis and thus the sample with respect to the beam in a  $\pm 5$  mm with 50 nm resolution. The goniometer, consist of a slotless direct drive torque motor from Aero-tech mounted on a customized helium/air bearing developed by Fluid Film Dynamics. The bearing can be fed by air or helium at 5.5 bar providing the same performance in terms of rigidity and runout.

On top of the goniometer, the sample centering stages (xyz) not only permit the sample centering with respect to the rotation axis but the creation of trayectories in combination with the  $\Omega$  axis (i.e. helical scans or raster scans). The stages, actuated by SMARACT piezo guides, are mounted on a titanium frame to minimize the thermal expansion. A precision slip ring, attached to the goniometer axis by a flexible coupling, permits transmitting the electrical signals to the connectors bellow.

The goniometer runout measurements, with air and with helium can be shown in the next Figure 7.

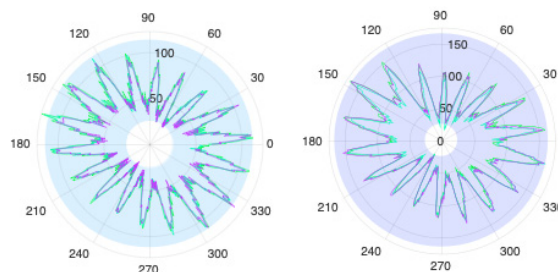


Figure 7: Run out measurements; 50 nm for goniometer with air (left) and 70 nm for the goniometer with He (right).

### On Axis Viewing System

The sample visualization is based on two separate optics, namely a high magnification and a low/medium magnification microscope. The high magnification branch includes a high-resolution objective with a fixed resolution of 0.7  $\mu\text{m}$ . The other branch, is a parallax-free commercial system (B-Zoom, ARINAX) composed of an objective with a 1mm diameter central hole and a splitter for 2 lens branches with 1.2  $\mu\text{m}$  resolution and  $> 1.2$   $\mu\text{m}$ , respectively. The two systems are located in parallel and a fast motorized stage permits changing from one to another in less than 4 s. This stage is located over a high resolution and stability vertical stage, which is mounted over the same XY stage of the goniometer to allow the alignment with respect to the beam.

## CONCLUSION

The design of the main white/pink beam optical elements and the end station have been presented, including the results that validate the performance of the cooling system of the HPM bender, the newly concept of the monochromator and the helium compatible diffractometer.

XAIRA beamline installation is foreseen to finished by the end of 2023. Further commissioning for optimization will be performed during this year.

## ACKNOWLEDGEMENTS

The authors acknowledge the team involved in the design, construction and commissioning of the beamline: XAIRA Beamline Staff, Isidro Crespo and Alejandro Enrique; Alignment Group, Marta Llonch and Jon Ladrera; Mechanical Workshop, Jose Ferrer, David Calderón, Karim Maimouni, Lluís Ginés and Oscar Borrego; Engineering, Marcos Quispe, Liudmila Nikitina, Yuri Nikitin and Núria Martí; Electronics Section, Bernat Molas, Xavi Serra, Antonio Camps and Alberto Ruz; Controls Section, José Centeno Ganbado, Oriol Vallcorba and Alberto Rubio; Nanomotion group, Juan Luis Friero.

## REFERENCES

- [1] J. Juanhuix *et al.*, “Optical design of the new microfocuss beamline BL06-XAIRA at ALBA”, in *AIP Conference Proc.*, vol. 2054, p. 060032, Jan. 2019.  
doi:10.1063/1.5084663
- [2] J. Campmany, J. Nicolás, J. Juanhuix, J. Marcos and V. Masana, “A general view of IDs to be installed at ALBA for

- second and third phase beam-lines,” in *AIP Conference Proc.*, vol. 1741, p. 020021, Jul. 2016.  
doi:10.1063/1.4952800
- [3] C. Colldelram, N. González, J. González, C. Ruget, J. Juanhuix and J. Nicolas, “Adaptive optics bender with sub-nanometer correction and stability”, in *AIP Conference Proc.*, vol. 2054, p. 060013, Jan. 2019.  
doi:10.1063/1.5084644
- [4] J. M. Alvarez, C. Colldelram, N. González, J. Juanhuix, J. Nicolas and I. Šics, “Design of monochromatic and white beam fluorescence screen monitors for XAIRA beamline at the Alba Synchrotron”, in *Proc. MEDSI'20*, Chicago, USA, Jul. 2021, pp. 249-251. doi:10.18429/JACoW-MEDSI2020-WEPA11
- [5] D. S. Morton, D. Cocco, N. M. Kelez, V. N. Srinivasan, P. M. Stefan and L. Zhang, “Design of a multipurpose mirror system for LCLS-2 photon transport studies (Conference Presentation)”, in *Proc. SPIE 9965, Adaptive X-Ray Optics IV*, 996506, Nov. 2016. doi:10.1117/12.2238784
- [6] M. Quispe *et al.*, “Design and fluid dynamics study of a recoverable helium sample environment system for optimal data quality in the new microfocus MX beamline at the Alba Synchrotron Light Source”, presented at MEDSI'23, Beijing, China, Nov. 2023, paper WEPPP035, this conference.